

Dynamic Tail Inference with Log-Laplace Volatility

Gordon V. Chavez*

University of California San Francisco

Abstract

We propose a family of stochastic volatility models that enable direct estimation of time-varying extreme event probabilities in time series with nonlinear dependence and power law tails. The models are a white noise process with conditionally log-Laplace stochastic volatility. In contrast to other, similar stochastic volatility formalisms, this process has an explicit, closed-form expression for its conditional probability density function, which enables straightforward estimation of dynamically changing extreme event probabilities. The process and volatility are conditionally Pareto-tailed, with tail exponent given by the reciprocal of the log-volatility's mean absolute innovation. These models thus can accommodate conditional power law-tail behavior ranging from very weakly non-Gaussian to Cauchy-like tails. Closed-form expressions for the models' conditional polynomial moments also allows for volatility modeling. We provide a straightforward, probabilistic method-of-moments estimation procedure that uses an asymptotic result for the process' conditional large deviation probabilities. We demonstrate the estimator's usefulness with a simulation study. We then give empirical applications to financial time series data, which show that this simple modeling method can be effectively used for dynamic tail inference in nonlinear, heavy-tailed time series.

Keywords: Stochastic volatility, Heavy tails, Extreme events, Nonlinear time series, Tail risk
AMS 2010 Subject Classification: 60G70, 62G32, 62M10, 62P05, 62P12, 91G70

*gordon.chavez@ucsf.edu

1 Introduction

Financial time series data is well-known to exhibit nonlinear dependence and “fat tails”. Such time series often display trends of increasing or decreasing volatility, along with a propensity for extreme values that is far greater than what would be predicted from a Gaussian or other distribution with finite polynomial moments. The latter observation was probably most famously addressed with the early Pareto-tailed and stable models for financial time series proposed by Mandelbrot (1963) and Fama (1968), while the most well-known early approaches to the nonlinear dependence problem were given by Engle (1982) and Bollerslev (1986) with original and generalized autoregressive conditional heteroskedasticity (ARCH, GARCH) models. Since then a great deal of research has been dedicated to extreme event probability estimation and nonlinear time series modeling for financial applications (e.g., Embrechts et. al. 2011 and Terasvirta et. al. 2010).

Estimation of extreme event probabilities is a very important problem for risk and portfolio management. Many estimators for the tail exponent of a marginal distribution have been proposed, e.g., by Hill (1975), Pickands (1975), and deHaan and Resnick (1980), however, these estimators are very sensitive to dependence in the data (Kearns and Pagan 1997, Diebold et. al. 2000). This makes them often ill-suited for application to many strongly dependent time series of interest for financial modeling, i.e., the squares and moduli of financial log-returns (Embrechts et. al. 2011 p. 270, 406). Relatedly, these estimators along with much of extreme value theory (EVT) are designed for inference of stationary, rather than time-varying, tail behavior. Gardes and Girard (2008) and Gardes and Stupfler (2014) have given nonparametric estimators for time-varying tail exponents, while Kelly (2014) has given a parametric approach to dynamic power law estimation in financial time series. The parametric modeling method we propose here, however, does not assume a time-varying tail exponent. Our approach is hence closer to McNeil and Frey’s (2000) combination of stationary EVT with GARCH modeling. However, we use a novel, stochastic volatility approach to enable such dynamic tail inference.

A canonical form of stochastic volatility model, first proposed by Taylor (1982, 1986), is given by

$$\varepsilon_t = \sigma_t z_t, \tag{1.1}$$

where z_t is an *i.i.d.* process with a mean of 0 and a variance of 1, and σ_t is a non-negative process defined by

$$\sigma_t = \exp(H_t), \tag{1.2}$$

where H_t is a Gaussian process with mean μ_H and variance $\sigma_H^2 < \infty$. An important example was the AR(1) model $H_t = \mu_H + \beta(H_{t-1} - \mu_H) + h_t$, where $\beta \in \mathbb{R}$ and $h_t \sim \mathcal{N}(0, \sigma_h^2)$ is *i.i.d.* The kind of model in (1.1) and (1.2), where H_t is a variety of Gaussian processes, has been extensively applied and studied, e.g., to exchange rate modeling by Harvey et. al. (1994) and extended to long-memory Gaussian H_t by Breidt et. al. (1998). However, the stochastic volatility σ_t in (1.2) follows a log-normal distribution, which has finite polynomial moments (see Johnson et. al. 1994). As a consequence, (1.1) also has bounded moments in the usual case of Gaussian z_t . This can be problematic for modeling time series with power law tails and divergent higher-order polynomial moments. Practically, such models will underestimate the probabilities of extreme events. To remedy this, z_t has often been chosen to follow the heavier-tailed Student’s t -distribution, e.g., in Harvey et. al. (1994), Liesenfeld and Jung (2000), and Chib et. al. (2002). However, with a Gaussian or Student’s t choice for z_t and Gaussian H_t , the model (1.1) does not have an explicit, closed-form expression for its conditional distributions. This makes estimation of model parameters as well as outcome probabilities difficult, often requiring the use of Bayesian and Monte Carlo methods such as those described in Jacquier et. al. (1994), Kim et. al. (1998), Sandmann and Koopman (1998),

or Chib et. al. (2002). Reliable estimation of similar, conditionally Student's t-distributed, ARCH-related models requires similar numerical procedures (see, e.g., Mousazadeh and Karimi 2007, Ardia 2008, Ardia and Hoogerheide 2010).

In this paper we propose a stochastic volatility formalism that enables straightforward and computationally inexpensive estimation of time-varying extreme event probabilities in time series with power law tail behavior. The models we present have the form (1.1)-(1.2), with $z_t \sim \mathcal{N}(0, 1)$. However, instead of defining (1.2)'s H_t as Gaussian, we make H_t conditionally *Laplace*-distributed, defining H_t as

$$H_t = E \{H_t | \mathcal{F}_{t-1}\} + h_t, \quad (1.3)$$

where \mathcal{F}_{t-1} is the filtration up to time $t - 1$ and h_t is *i.i.d.* Laplace-distributed with density

$$p_h(h_t) = \frac{1}{2\Delta} \exp\left(-\frac{|h_t|}{\Delta}\right), \quad (1.4)$$

where $\Delta > 0$. This simple but important adjustment endows (1.1)-(1.2)'s σ_t and ε_t with power law-tailed conditional probability density functions, for which there are closed-form expressions. These conditional densities give the result

$$P\{|\varepsilon_t| \geq \Lambda | \mathcal{F}_{t-1}\} \sim f(\Delta) \exp\left(\frac{E\{H_t | \mathcal{F}_{t-1}\}}{\Delta}\right) \Lambda^{-1/\Delta} \quad (1.5)$$

as $\Lambda \rightarrow \infty$. Hence H_t 's mean absolute innovation Δ specifies the tail exponent, which allows (1.1)-(1.4) to flexibly define processes ranging from only mildly non-Gaussian with $\Delta \approx 0$ to processes with Cauchy-like tails at $\Delta = 1$. The process ε_t 's tail probabilities are also strongly and explicitly dependent on the process H_t , which enables their dynamic estimation. We give a simple, probabilistic method-of-moments estimation procedure for the tail exponent, which takes advantage of the result (1.5) for ε_t 's tail probabilities. We then present a simulation study and empirical applications to S&P 500 Index data, U.S. Dollar/Euro foreign exchange rate data, and Bitcoin Price Index data, which show that this modeling method can be effective for dynamic estimation of volatility and extreme event probabilities in nonlinear, power law-tailed time series. We give some concluding remarks, an appendix with proofs of the main results, and a second appendix, which shows that very similar results, including (1.5), can also be derived for the case when z_t is Laplace-distributed. We lastly give a third appendix with empirical applications to urban air pollution data and solar activity data.

2 Model

We will denote H_t 's conditional expectation as $\bar{H}_t = E\{H_t | \mathcal{F}_{t-1}\}$. We first give expressions for σ_t 's conditional probability density and ε_t 's conditional polynomial moments.

Lemma 2.1. *Given (1.3)-(1.4), σ_t in (1.2) is conditionally distributed according to the log-Laplace probability density function*

$$p_\sigma(\sigma_t | \mathcal{F}_{t-1}) = \begin{cases} \frac{1}{2\Delta} \exp\left(-\frac{\bar{H}_t}{\Delta}\right) \sigma_t^{1/\Delta-1}; & 0 < \sigma_t < \exp(\bar{H}_t) \\ \frac{1}{2\Delta} \exp\left(\frac{\bar{H}_t}{\Delta}\right) \sigma_t^{-1/\Delta-1}; & \sigma_t \geq \exp(\bar{H}_t) \end{cases} \quad (2.1)$$

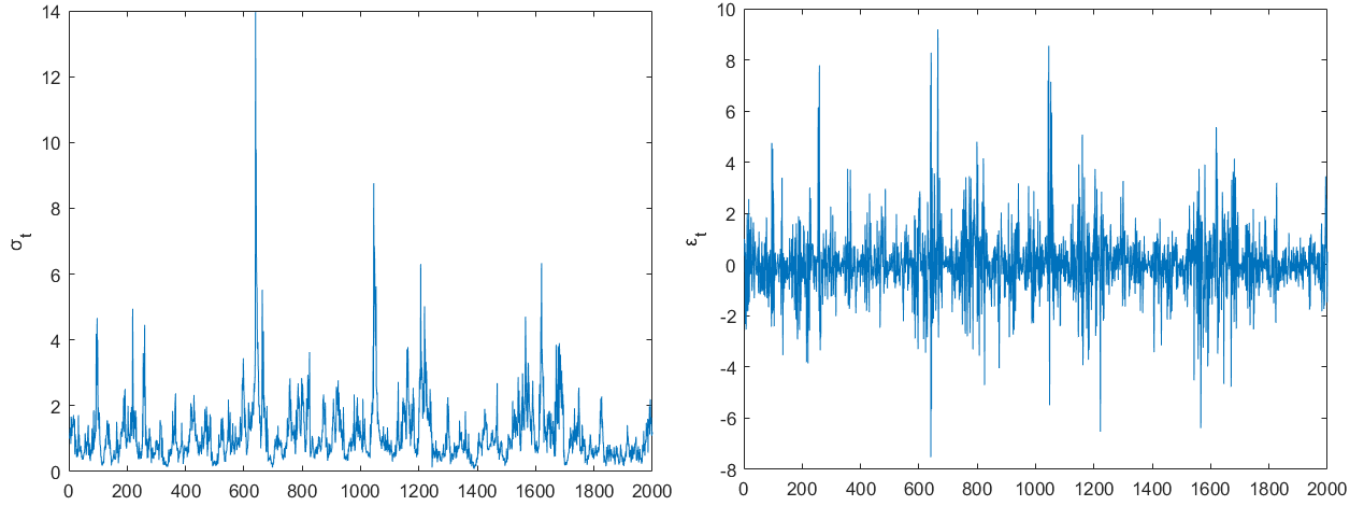


Figure 1: A typical realization of the stochastic volatility σ_t defined in (1.2)-(1.4) and (1.1)'s corresponding process ε_t with $z_t \sim \mathcal{N}(0, 1)$, $H_t = .5H_{t-1} + .4H_{t-2} + h_t$, and $\Delta = 1/4$.

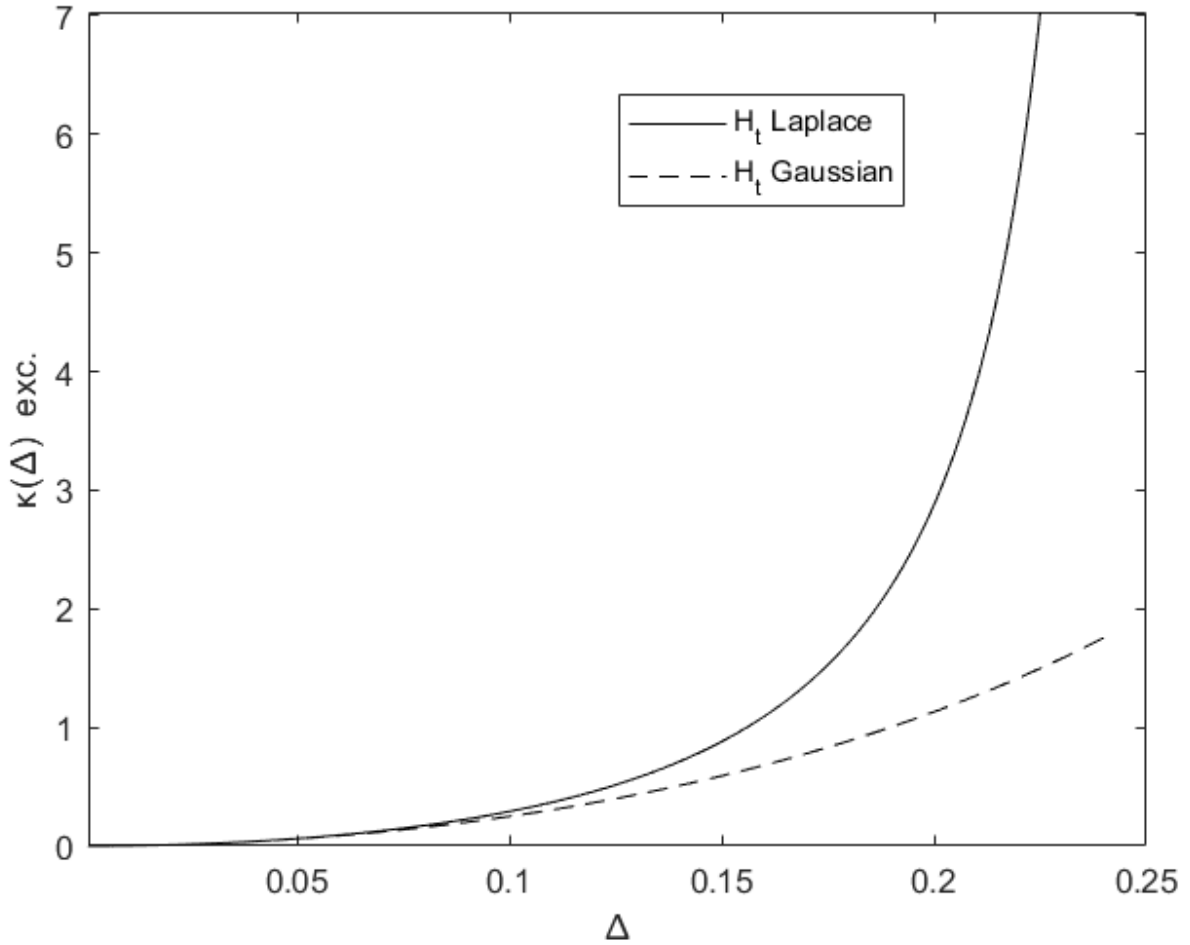


Figure 2: A graph of (2.3)'s conditional excess kurtosis $\kappa^{\text{exc.}}(\Delta) = \kappa(\Delta) - 3$ for Laplace H_t (Solid) along with the corresponding result for Gaussian H_t (Dashed).

Corollary 2.1. *Given (1.1) and (2.1) with $z_t \sim \mathcal{N}(0, 1)$, for all even $n \geq 2$, for $\Delta \geq 1/n$, $E\{\varepsilon_t^n | \mathcal{F}_{t-1}\} = \infty$, while for $\Delta < 1/n$,*

$$E\{\varepsilon_t^n | \mathcal{F}_{t-1}\} = \exp(n\bar{H}_t) \frac{(n-1)!!}{1 - n^2\Delta^2}. \quad (2.2)$$

Several graphs of (2.1) are given in Fig. 3. We note from Corollary 2.1 that the conditional kurtosis $\kappa_t = E\{\varepsilon_t^4 | \mathcal{F}_{t-1}\} / (E\{\varepsilon_t^2 | \mathcal{F}_{t-1}\})^2$ diverges or is not well-defined for $\Delta \geq 1/4$. However, when (2.2) is used to calculate κ_t for $\Delta < 1/4$, it can be easily shown that the conditional kurtosis has the time-independent definition

$$\kappa(\Delta) = 3 \frac{(1 - 4\Delta^2)^2}{1 - 16\Delta^2}, \quad (2.3)$$

which is minimized at $\kappa(0) = 3$, the Gaussian kurtosis. The divergent algebraic structure of (2.3) contrasts with the kurtosis' exponential structure for Gaussian H_t , which would be given by $\kappa_t = 3 \exp(8\Delta^2)$. The *excess kurtosis* $\kappa^{\text{exc.}}(\Delta) = \kappa(\Delta) - 3$ is graphed in Fig. 2 for both Laplace and Gaussian H_t . Now that we have given ε_t 's conditional moment structure, we will present its conditional probability density function and characterize its near-mean and tail behavior.

Theorem 2.1. *Given (2.1) with $z_t \sim \mathcal{N}(0, 1)$, (1.1)'s ε_t is distributed according to the conditional probability density function*

$$p_\varepsilon(\varepsilon_t | \mathcal{F}_{t-1}) = \frac{1}{4\sqrt{\pi}\Delta} \left(\sqrt{2}e^{\bar{H}_t}\right)^{-1/\Delta} \Gamma\left(\frac{1-1/\Delta}{2}, \frac{\varepsilon_t^2}{2e^{2\bar{H}_t}}\right) |\varepsilon_t|^{1/\Delta-1} \\ + \frac{1}{4\sqrt{\pi}\Delta} \left(\sqrt{2}e^{\bar{H}_t}\right)^{1/\Delta} \gamma\left(\frac{1+1/\Delta}{2}, \frac{\varepsilon_t^2}{2e^{2\bar{H}_t}}\right) |\varepsilon_t|^{-1/\Delta-1} \quad (2.4)$$

where

$$\Gamma(a, b) = \int_b^\infty x^{a-1} e^{-x} dx \quad (2.5)$$

is the upper incomplete gamma function and

$$\gamma(a, b) = \int_0^b x^{a-1} e^{-x} dx \quad (2.6)$$

is the lower incomplete gamma function.

Several graphs of (2.4) are given in Fig. 3. Note that with larger Δ and smaller \bar{H}_t the densities are more sharply peaked around the origin. This can also be seen from the following result.

Corollary 2.2. *For $\Delta < 1$, as $|\varepsilon_t| \rightarrow 0$,*

$$p_\varepsilon(\varepsilon_t | \mathcal{F}_{t-1}) \sim \frac{1}{\sqrt{2\pi}e^{\bar{H}_t}} \frac{1}{1 - \Delta^2}. \quad (2.7)$$

It can be seen in the proof of Theorem 2.1 that the piece-wise structure of (2.1) gives (2.4) a structure involving two power law terms. We will show that the second of these terms is the primary driver of ε_t 's tail behavior.

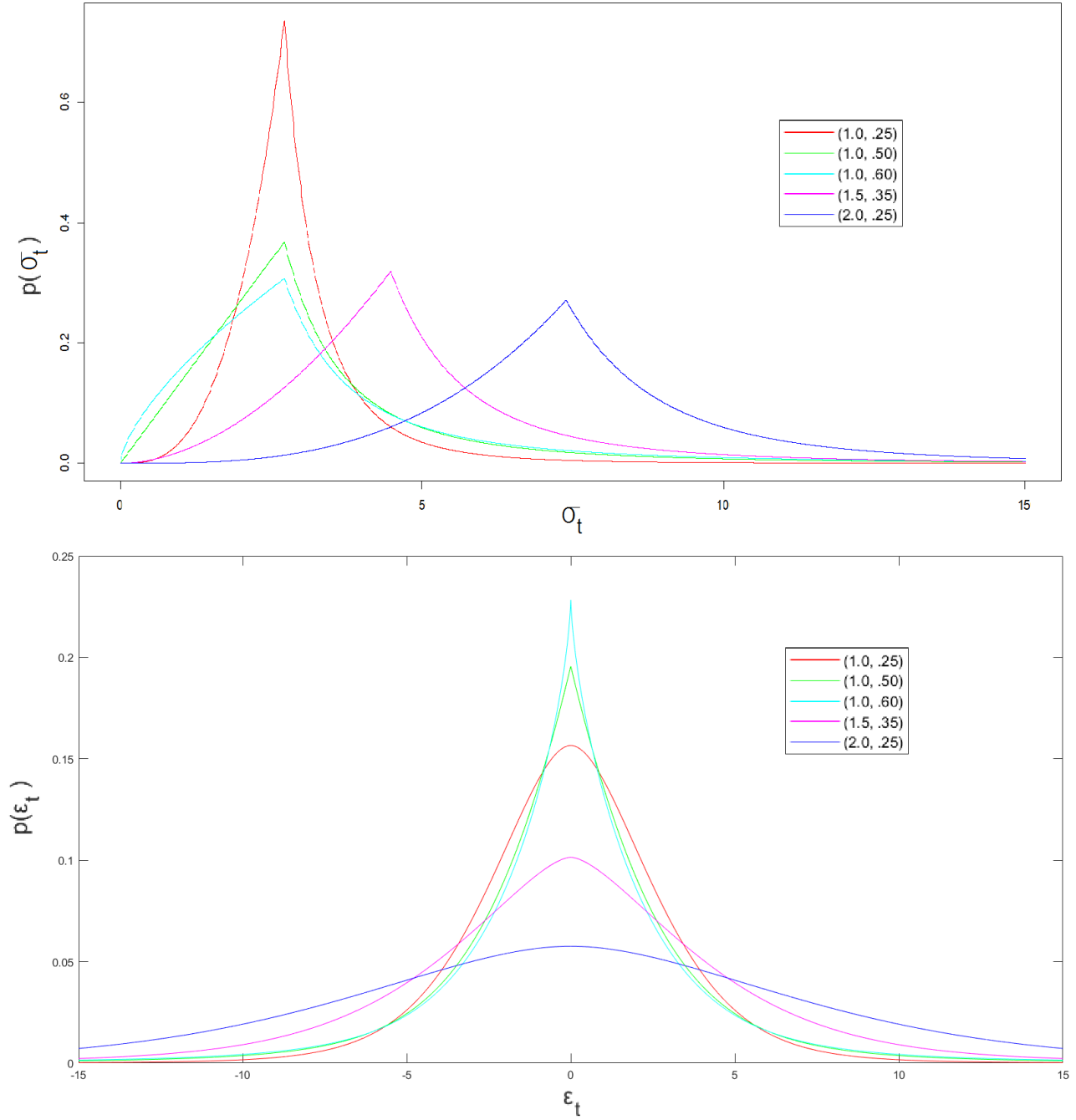


Figure 3: Graphs of the probability density functions (2.1) (Top) and (2.4) (Bottom) with (\bar{H}_t, Δ) equal to (1, .25) in Red, (1, .50) in Green, (1, .60) in Cyan, (1.5, .35) in Magenta, and (2, .25) in Blue.

Corollary 2.3. By (2.4) and (2.1), as $\Lambda \rightarrow \infty$,

$$\begin{aligned} P\{|\varepsilon_t| \geq \Lambda | \mathcal{F}_{t-1}\} &\sim \frac{\sqrt{2}^{1/\Delta}}{2\sqrt{\pi}} \Gamma\left(\frac{1+1/\Delta}{2}\right) \exp\left(\frac{\bar{H}_t}{\Delta}\right) \Lambda^{-1/\Delta} \\ &= \frac{\sqrt{2}^{1/\Delta}}{\sqrt{\pi}} \Gamma\left(\frac{1+1/\Delta}{2}\right) P\{\sigma_t \geq \Lambda | \mathcal{F}_{t-1}\}. \end{aligned} \quad (2.8)$$

We will make extensive use of (2.8)'s first line in our estimation procedure described in the next section. Note that (2.8)'s dependence on \bar{H}_t has the form $\exp(\bar{H}_t/\Delta)$. This shows that with larger Δ , ε_t 's asymptotic tail probabilities are less responsive to the conditional, low-order moment behavior encapsulated in \bar{H}_t and hence these tail probabilities are more completely determined by the stationary structure given by Δ .

The second line of (2.8) shows that ε_t 's asymptotic large deviation probabilities are simply proportional to σ_t 's corresponding probabilities through a Δ -dependent factor. Note that $\Gamma(3/2) = \sqrt{\pi}/2$ and $\Gamma(1/2) = \sqrt{\pi}$, therefore (2.8)'s second line reduces to simply

$$P\{|\varepsilon_t| \geq \Lambda | \mathcal{F}_{t-1}\} \sim P\{\sigma_t \geq \Lambda | \mathcal{F}_{t-1}\}$$

for $\Delta = 1/2$ and as $\Delta \rightarrow \infty$. Now that we have presented the model's polynomial moments and probabilistic structure, we will describe an estimation procedure using some of the above results.

3 Estimation

We begin by considering the conditional expectation of the unobservable quantity H_t , given the value of the observable $\log |\varepsilon_t|$.

Proposition 3.1. Given (1.1) and (1.2),

$$E\{H_t | \log |\varepsilon_t|\} = \log |\varepsilon_t| + \frac{\log 2 + \gamma}{2} \approx \log |\varepsilon_t| + .6352, \quad (3.1)$$

where

$$\gamma = \lim_{n \rightarrow \infty} \left(\sum_{k=1}^n \frac{1}{k} - \log n \right) \approx .5772$$

is the Euler-Mascheroni constant.

By Proposition 3.1, an unbiased estimator for H_t is given by

$$\hat{H}_t = \log |\varepsilon_t| + \frac{\log 2 + \gamma}{2} \approx \log |\varepsilon_t| + .6352. \quad (3.2)$$

An arbitrary regression model $m(\cdot)$ for estimation of $E\{H_t | \mathcal{F}_{t-1}\}$ may then be trained using the \hat{H}_t 's and any other relevant variables, giving

$$\hat{\hat{H}}_t = \hat{E}\{H_t | \mathcal{F}_{t-1}\} = m\left(\hat{H}_{t-1}, \dots, \hat{H}_{t-p}, \dots\right). \quad (3.3)$$

We then estimate Δ by finding an approximate solution to the empirical, probabilistic moment constraint

$$\frac{1}{T} \sum_{t=1}^T \mathbb{1}(|\varepsilon_t| \geq \Lambda) = \frac{1}{T} \sum_{t=1}^T \int_{\Lambda}^{\infty} 2p_{\varepsilon}\left(\varepsilon | \hat{\hat{H}}_t, \hat{\Delta}\right) d\varepsilon, \quad (3.4)$$

where $p_\varepsilon(\cdot)$ is given in (2.4) and $\Lambda \in \mathbb{R}^+$. The constraint (3.4) is justified by the law of total expectation, which requires that $E\{\mathbb{1}(|\varepsilon_t| \geq \Lambda)\} = E\{E\{\mathbb{1}(|\varepsilon_t| \geq \Lambda) | \mathcal{F}_{t-1}\}\}$. This Δ -estimation method requires an approximation of the integral on the right-hand side of (3.4). We will approximate (3.4)'s integral with the asymptotic result (2.8), which is a justifiable approximation for sufficiently large Λ . We then use the estimator

$$\hat{\Delta}(\Lambda) = \operatorname{argmin}_{\Delta} \left\{ \left| \sum_{t=1}^T \left(\mathbb{1}(|\varepsilon_t| \geq \Lambda) - \frac{\sqrt{2}^{1/\Delta}}{2\sqrt{\pi}} \Gamma\left(\frac{1+1/\Delta}{2}\right) \exp\left(\frac{\hat{H}_t}{\Delta}\right) \Lambda^{-1/\Delta} \right) \right| \right\} \quad (3.5)$$

In the simulation and empirical sections below, we search for (3.5)'s $\hat{\Delta}$ over the range $[\cdot 01, 1]$ with a precision of $\cdot 01$.

4 Simulation

In this section we present results of the estimation procedure described in the previous section for simulations of the process (1.1)-(1.4). We run 1000 simulations each, with sample sizes of 625 and 1250, for Δ ranging from $\cdot 05$ to $\cdot 50$. The model used for (3.3)'s \hat{H}_t is a linear autoregressive model that uses the 10 previous values of (3.2)'s \hat{H}_t . This AR(10) model is calibrated using the Yule-Walker method.

We present simulation results for two different, simple processes for H_t . The first is given by the AR(2) process

$$H_t = \cdot 5H_{t-1} + \cdot 4H_{t-2} + h_t \quad (4.1)$$

and the second is given by the AR(5) process

$$H_t = \cdot 05H_{t-1} + \cdot 05H_{t-2} + \cdot 25H_{t-3} + \cdot 2H_{t-4} + \cdot 35H_{t-5} + h_t. \quad (4.2)$$

The results are presented in Table 1, where we give the averages and standard deviations of $\hat{\Delta}$ over the 1000 simulations. For Λ , we choose $2\hat{\sigma}_\varepsilon$, $3\hat{\sigma}_\varepsilon$, and $4\hat{\sigma}_\varepsilon$, where $\hat{\sigma}_\varepsilon^2$ is ε_t 's sample variance. This gives a set of data-driven Λ values for which (2.8) is an increasingly accurate approximation of (3.4)'s integral.

One can see in Table 1 that for H_t given by (4.1) (resp. (4.2)) that for $\Delta \leq \cdot 30$ (resp. $\cdot 25$), $\hat{\Delta}(k\hat{\sigma}_\varepsilon)$'s bias appears to decrease as k increases, while for $\Delta > \cdot 30$ (resp. $\cdot 25$) the bias seems to remain constant or slightly increase with k . The estimator's variance appears to nearly always increase with k , which is likely due to the higher variance in probability estimates for larger deviations. It is also clear that the variance increases with Δ , which could be related to the increased variance in $\hat{\sigma}_\varepsilon$ for larger Δ . Doubling the sample size decreased the estimators' standard deviations by $\cdot 01$ to $\cdot 02$, and had a similar effect on the some of the biases. Although the bias actually increased in many cases by increasing the sample size.

The estimator $\hat{\Delta}(2\hat{\sigma}_\varepsilon)$'s bias is very large for small Δ and decreases greatly as $\Delta \rightarrow 1/2$. This is possibly because as Δ increases, (2.4) becomes sharper around the origin, and hence $2\hat{\sigma}_\varepsilon$ is sufficiently far in the tails for (2.8) to be a good approximation to (3.4)'s integral. Meanwhile for $k = 3$ and 4 , $\hat{\Delta}(k\hat{\sigma}_\varepsilon)$'s bias appears to be minimal around $\cdot 10 \leq \Delta \leq \cdot 2$. The inherent upward bias in the $\hat{\Delta}$'s is likely due to model error in \hat{H}_t , since decreased predictability of H_t manifests as a higher empirical Δ . This explains the increases in bias seen when doubling the sample size, because the AR(10) models for \hat{H}_t overfitted the data less on the larger samples.

The processes (4.1)-(4.2) were selected for their simplicity and the superficial similarity between their short-term autocorrelation structure and those of the first two empirical applications in the

Table 1: Estimation results using (3.5)'s $\hat{\Delta}(\Lambda)$, averaged over 1000 simulations of T samples of (1.1)-(1.4) with H_t given by (4.1) and (4.2). Model for (3.3)'s \hat{H}_t is AR(10).

$H_t = (4.1)$											
$T = 625 - 10$											
Δ	.05	.10	.15	.20	.25	.30	.35	.40	.45	.50	
avg. $\hat{\Delta}(2\hat{\sigma}_\varepsilon)$.28	.27	.28	.31	.35	.39	.43	.47	.50	.55	
avg. $\hat{\Delta}(3\hat{\sigma}_\varepsilon)$.14	.16	.20	.26	.32	.37	.41	.47	.51	.56	
avg. $\hat{\Delta}(4\hat{\sigma}_\varepsilon)$.10	.13	.19	.26	.31	.36	.42	.47	.51	.56	
std. dev. $\hat{\Delta}(2\hat{\sigma}_\varepsilon)$.02	.03	.04	.05	.06	.07	.08	.09	.11	.13	
std. dev. $\hat{\Delta}(3\hat{\sigma}_\varepsilon)$.02	.03	.06	.07	.09	.10	.11	.13	.14	.15	
std. dev. $\hat{\Delta}(4\hat{\sigma}_\varepsilon)$.03	.05	.07	.08	.09	.11	.12	.13	.14	.16	
$T = 1250 - 10$											
Δ	.05	.10	.15	.20	.25	.30	.35	.40	.45	.50	
avg. $\hat{\Delta}(2\hat{\sigma}_\varepsilon)$.26	.25	.27	.30	.34	.38	.41	.45	.50	.54	
avg. $\hat{\Delta}(3\hat{\sigma}_\varepsilon)$.13	.15	.21	.27	.32	.37	.41	.46	.51	.55	
avg. $\hat{\Delta}(4\hat{\sigma}_\varepsilon)$.09	.14	.21	.26	.32	.38	.42	.47	.52	.56	
std. dev. $\hat{\Delta}(2\hat{\sigma}_\varepsilon)$.01	.02	.02	.03	.04	.05	.06	.08	.09	.11	
std. dev. $\hat{\Delta}(3\hat{\sigma}_\varepsilon)$.01	.03	.06	.07	.08	.09	.10	.11	.12	.14	
std. dev. $\hat{\Delta}(4\hat{\sigma}_\varepsilon)$.02	.05	.06	.07	.08	.09	.10	.12	.14	.14	
$H_t = (4.2)$											
$T = 625 - 10$											
Δ	.05	.10	.15	.20	.25	.30	.35	.40	.45	.50	
avg. $\hat{\Delta}(2\hat{\sigma}_\varepsilon)$.29	.27	.26	.26	.28	.32	.36	.41	.46	.52	
avg. $\hat{\Delta}(3\hat{\sigma}_\varepsilon)$.15	.14	.17	.21	.26	.32	.38	.43	.48	.52	
avg. $\hat{\Delta}(4\hat{\sigma}_\varepsilon)$.10	.11	.15	.20	.26	.32	.37	.42	.48	.53	
std. dev. $\hat{\Delta}(2\hat{\sigma}_\varepsilon)$.02	.02	.03	.03	.05	.07	.09	.10	.12	.12	
std. dev. $\hat{\Delta}(3\hat{\sigma}_\varepsilon)$.02	.02	.04	.06	.08	.08	.09	.10	.10	.12	
std. dev. $\hat{\Delta}(4\hat{\sigma}_\varepsilon)$.02	.04	.06	.07	.08	.08	.08	.09	.10	.11	
$T = 1250 - 10$											
Δ	.05	.10	.15	.20	.25	.30	.35	.40	.45	.50	
avg. $\hat{\Delta}(2\hat{\sigma}_\varepsilon)$.27	.26	.25	.25	.27	.32	.36	.41	.46	.52	
avg. $\hat{\Delta}(3\hat{\sigma}_\varepsilon)$.13	.13	.17	.23	.28	.33	.38	.43	.48	.53	
avg. $\hat{\Delta}(4\hat{\sigma}_\varepsilon)$.09	.11	.16	.22	.28	.33	.38	.43	.48	.53	
std. dev. $\hat{\Delta}(2\hat{\sigma}_\varepsilon)$.01	.02	.02	.03	.05	.06	.08	.09	.10	.11	
std. dev. $\hat{\Delta}(3\hat{\sigma}_\varepsilon)$.01	.02	.05	.06	.07	.07	.08	.08	.09	.10	
std. dev. $\hat{\Delta}(4\hat{\sigma}_\varepsilon)$.02	.04	.05	.06	.06	.07	.07	.08	.08	.10	

next section. In particular, (4.1) and (4.2)'s $|\varepsilon_t|$ processes appear to be slightly more strongly locally correlated, but otherwise their short-term autocorrelations resemble those seen in the first and second empirical applications respectively. These simulations hence show that with a realistically sized sample and similar conditions to the applications below, $\hat{\Delta}(k\hat{\sigma}_\varepsilon)$ with $k = 3$ or 4 can provide a computationally inexpensive and satisfactory estimate of Δ , given a predictive model for H_t .

5 Empirical Application

In this section we apply our modeling and estimation procedure to three financial time series data sets. The first data set is the daily log-returns of the S&P 500 Index (SPX) from January 17th, 2013 to December 7th, 2018. One day where the log-return was zero has been removed, giving a total of 1,483 samples over approximately 6 years. The second data set is the daily log-returns of the U.S. Dollar/Euro foreign exchange rate (USD/EUR) from November 5th, 2013 to October 19th, 2018. This foreign exchange rate data was retrieved from the Federal Reserve Bank of St. Louis, and 46 days where no data was available have been removed, along with 14 days where the log-return was zero, giving a total of 1,228 samples over approximately 5 years. The third data set is the daily log-returns of the Bitcoin Price Index (BPI) from October 12th, 2013 to November 19th, 2018, which comprises 1,863 samples over approximately 5 years.

For all three data sets we use the same regression method for (3.3)'s \hat{H}_t . This method proceeds by applying Principal Component Analysis (PCA) to $\left\{\hat{H}_{t-1}, \dots, \hat{H}_{t-10}\right\}_{t=11}^{T+10}$ to create the uncorrelated Principal Components (PCs) $\phi_t^{(1)}, \dots, \phi_t^{(10)}$. We then use Tibshirani's (1996) LASSO regression and Friedman et. al.'s (2010) cyclic coordinate descent to give the model

$$\hat{H}_t = \hat{\beta}_0 + \sum_{n=1}^{10} \hat{\beta}_n \phi_t^{(n)}, \quad (5.1)$$

where

$$\hat{\beta} = \operatorname{argmin}_{\beta} \left\{ \frac{1}{2T} \sum_{t=11}^{T+10} \left| \hat{H}_t - \beta_0 - \sum_{n=1}^{10} \beta_n \phi_t^{(n)} \right|^2 + \lambda \sum_{n=1}^{10} |\beta_n| \right\}, \quad (5.2)$$

and λ minimizes \hat{H}_t 's mean absolute 10-fold cross-validation error. This procedure, which can be called L1-penalized PC Regression, gives a sparse, linear, autoregressive model of order 10 for \hat{H}_t . We will use this simple model with (3.5)'s $\hat{\Delta} = \hat{\Delta}(4\hat{\sigma}_\varepsilon)$ to give an estimate of ε_t 's next-day volatility $\bar{\sigma}_{\varepsilon,t} = \sqrt{E\{\varepsilon_t^2 | \mathcal{F}_{t-1}\}}$ as well as a dynamic estimate of the probability that $|\varepsilon_t| \geq 3\hat{\sigma}_\varepsilon$.

We use the moment result (2.2) to give the following model for the next-day volatility:

$$\hat{\sigma}_{\varepsilon,t} = \sqrt{E\{\varepsilon_t^2 | \hat{H}_t, \hat{\Delta}\}} = \exp\left(\hat{H}_t\right) \sqrt{\frac{1}{1 - 4\hat{\Delta}^2}}. \quad (5.3)$$

We additionally use the asymptotic result (2.8) to give the dynamic probability estimate

$$\hat{P}\left\{|\varepsilon_t| \geq 3\hat{\sigma}_\varepsilon | \hat{H}_t, \hat{\Delta}\right\} = \frac{\sqrt{2^{1/\hat{\Delta}}}}{2\sqrt{\pi}} \Gamma\left(\frac{1 + 1/\hat{\Delta}}{2}\right) \exp\left(\frac{\hat{H}_t}{\hat{\Delta}}\right) (3\hat{\sigma}_\varepsilon)^{-1/\hat{\Delta}}. \quad (5.4)$$

To assess the linear predictive capability of (5.3)-(5.4) we use the empirical correlations

$$\rho_{|\varepsilon|, \hat{\sigma}} = \operatorname{corr}\left\{|\varepsilon_t|, \hat{\sigma}_{\varepsilon,t}\right\} \quad (5.5)$$

and

$$\rho_{|\varepsilon|, \hat{P}} = \text{corr} \left\{ |\varepsilon_t|, \hat{P} \left\{ |\varepsilon_t| \geq 3\hat{\sigma}_\varepsilon | \hat{H}_t, \hat{\Delta} \right\} \right\}. \quad (5.6)$$

To more closely evaluate the predictiveness of (5.4), we first note that the stationary probability that $|\varepsilon_t| \geq 3\hat{\sigma}_\varepsilon$ under a Gaussian distribution is $\approx .0027$. We then use (5.4) to define a binary classifier ξ_t with the form

$$\xi_t = \begin{cases} 1; & \hat{P} \left\{ |\varepsilon_t| \geq 3\hat{\sigma}_\varepsilon | \hat{H}_t, \hat{\Delta} \right\} \geq 5 \times .0027 \\ 0; & \hat{P} \left\{ |\varepsilon_t| \geq 3\hat{\sigma}_\varepsilon | \hat{H}_t, \hat{\Delta} \right\} < 5 \times .0027 \end{cases} \quad (5.7)$$

Hence ξ_t identifies days when the probability that $|\varepsilon_t| \geq 3\hat{\sigma}_\varepsilon$ exceeds 5 times the stationary Gaussian probability. We then calculate ξ_t 's sensitivity (Sn.) and specificity (Sp.), which are defined here as

$$\text{Sn.} = \frac{|\{\varepsilon_t \text{ s.t. } |\varepsilon_t| \geq 3\hat{\sigma}_\varepsilon \wedge \xi_t = 1\}|}{|\{\varepsilon_t \text{ s.t. } |\varepsilon_t| \geq 3\hat{\sigma}_\varepsilon\}|} \quad (5.8)$$

and

$$\text{Sp.} = \frac{|\{\varepsilon_t \text{ s.t. } |\varepsilon_t| < 3\hat{\sigma}_\varepsilon \wedge \xi_t = 0\}|}{|\{\varepsilon_t \text{ s.t. } |\varepsilon_t| < 3\hat{\sigma}_\varepsilon\}|}. \quad (5.9)$$

Empirical results for (3.5)'s $\hat{\Delta}(4\hat{\sigma}_\varepsilon)$, as well as test results for (5.5)-(5.6), and (5.8)-(5.9) are given in Table 2 for the SPX, USD/EUR, and BPI applications. These results are averaged over 100 random train/test splits of the datasets $\left\{ \hat{H}_t, \hat{H}_{t-1}, \dots, \hat{H}_{t-10} \right\}_{t=11}^{T+10}$ for several different ratios of training sample size N_{Train} to testing sample size N_{Test} , ranging from 50/50 to 90/10.

We begin by noting that for the SPX data, $\hat{\Delta} \approx .30$, while for the USD/EUR data the tail is estimated to be much lighter with $\hat{\Delta} \approx .19$. The BPI data's tail is estimated to be the heaviest with $\hat{\Delta} \approx .38$. The classifier defined with (5.4) and (5.7) is clearly predictive on the test sets for all applications. In the SPX and BPI data, ξ_t can correctly identify $> 80\%$ of days where $|\varepsilon_t| \geq 3\hat{\sigma}_\varepsilon$, while in the USD/EUR data, ξ_t performs less well but is still predictive with about 60% of such days correctly identified. These sensitivities would be much lower under a less heavy-tailed model. For all three data sets ε_t had high specificities of about 67%, 72%, and 60% respectively. This gives ξ_t a *balanced accuracy* or *non-error rate*, defined as $(\text{Sn.} + \text{Sp.})/2$, of about 72% for the SPX and BPI, and 65% for the USD/EUR. Meanwhile the average test correlation between (5.3)'s volatility estimate $\hat{\sigma}_{\varepsilon,t}$ and $|\varepsilon_t|$ is 28-30% for the SPX, 24-25% for the USD/EUR, and 37% for the BPI.

We note that since the model (5.1)-(5.2) uses the 10 previous values of (3.2)'s \hat{H}_t , it has a memory length of about two trading weeks. This relatively naive, short-memory modeling of H_t can likely be improved for these applications, since many researchers have found empirical evidence of long-memory in SPX volatility (see Ding et. al. 1993, Bollerslev and Mikkelsen 1996, Lobato and Savin 1998, Ray and Tsay 2000, Grau-Carles 2000) and foreign exchange rate volatility (see Andersen et. al. 2001, Gencay et. al. 2001). The modeling could also be adjusted to accomodate the asymmetric tails observed in stock market data, often called the "leverage effect" (see Black 1976, Christie 1982, Nelson 1991, Engle and Ng 1993). Overall, though, the study here shows that a simple, short-memory model for H_t with the parametrization (1.1)-(1.5) can enable computationally inexpensive and straightforward dynamic tail inference in time series data. Plots of the SPX, USD/EUR, and BPI data along with corresponding volatility and probability estimates are given in Fig.4.

Table 2: Empirical Application Results:

Averages are calculated from 100 random train/test splits for each row.

SPX						
$N_{\text{Train}}/N_{\text{Test}}$		avg. $\widehat{\Delta}(4\widehat{\sigma}_\varepsilon)$	avg. $\rho_{ \varepsilon ,\widehat{\sigma}}$	avg. $\rho_{ \varepsilon ,\widehat{P}}$	avg. Sn.	avg. Sp.
741/742	(50/50)	.284	.280	.263	.717	.677
889/594	(60/40)	.293	.284	.273	.749	.682
1,038/445	(70/30)	.299	.286	.281	.751	.673
1,186/297	(80/20)	.304	.290	.285	.778	.667
1,334/149	(90/10)	.301	.296	.290	.823	.663
USD/EUR						
$N_{\text{Train}}/N_{\text{Test}}$		avg. $\widehat{\Delta}(4\widehat{\sigma}_\varepsilon)$	avg. $\rho_{ \varepsilon ,\widehat{\sigma}}$	avg. $\rho_{ \varepsilon ,\widehat{P}}$	avg. Sn.	avg. Sp.
614/614	(50/50)	.183	.240	.195	.538	.731
736/492	(60/40)	.191	.248	.213	.556	.715
859/369	(70/30)	.184	.252	.215	.569	.722
982/246	(80/20)	.190	.252	.217	.582	.718
1,105/123	(90/10)	.197	.252	.225	.633	.724
BPI						
$N_{\text{Train}}/N_{\text{Test}}$		avg. $\widehat{\Delta}(4\widehat{\sigma}_\varepsilon)$	avg. $\rho_{ \varepsilon ,\widehat{\sigma}}$	avg. $\rho_{ \varepsilon ,\widehat{P}}$	avg. Sn.	avg. Sp.
931/932	(50/50)	.384	.372	.333	.839	.593
1,117/746	(60/40)	.371	.370	.322	.829	.610
1,304/559	(70/30)	.375	.375	.330	.833	.602
1,490/373	(80/20)	.376	.371	.329	.830	.606
1,676/187	(90/10)	.379	.365	.323	.827	.603

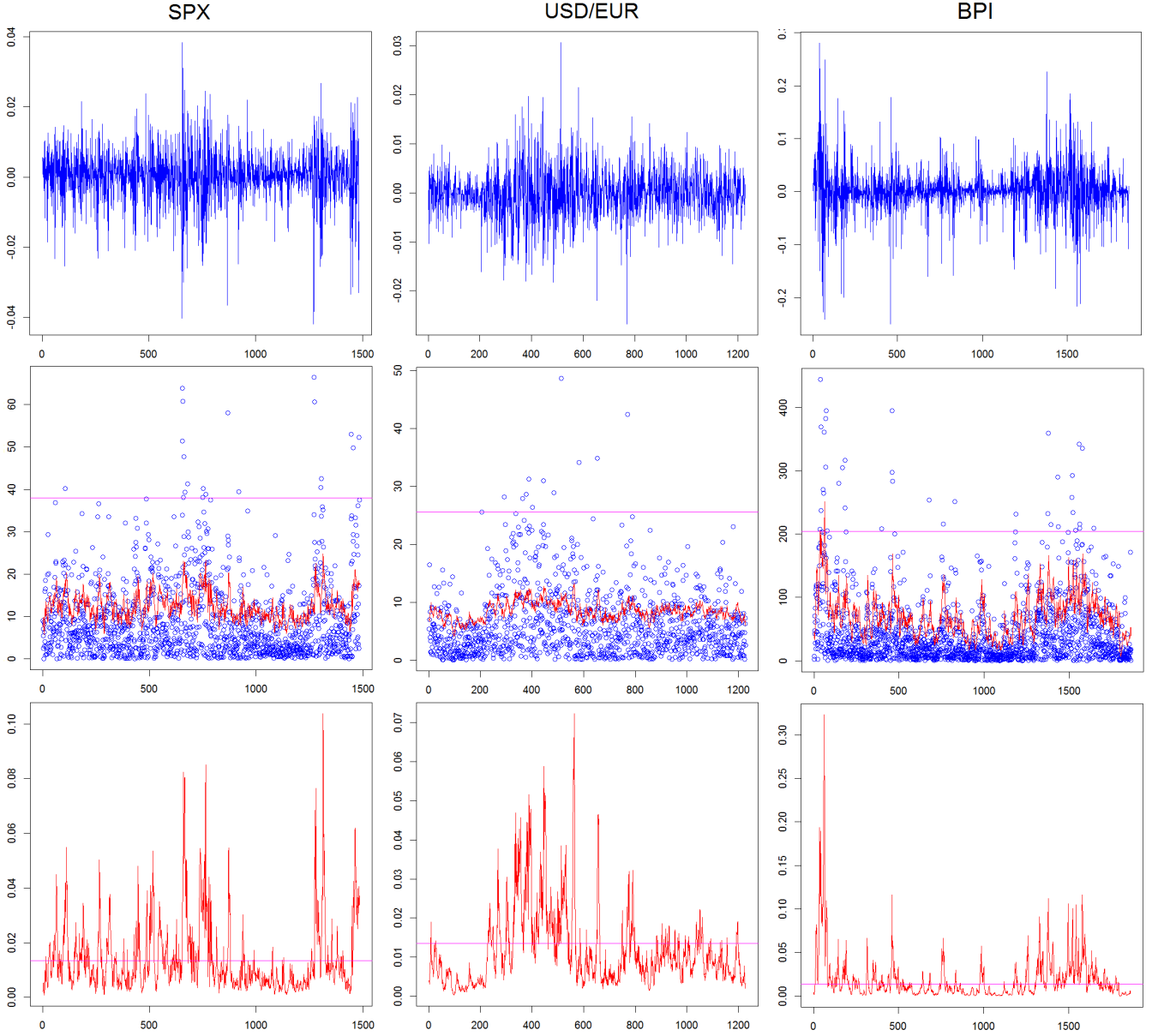


Figure 4: Top Row: Plots of the log-returns ε_t for the SPX, USD/EUR, and BPI. Middle Row: Plots of annualized $|\varepsilon_t|$ in Blue and (5.3)'s $\hat{\sigma}_{\varepsilon,t}$ in Red for the SPX, USD/EUR, and BPI with $3\hat{\sigma}_\varepsilon$ marked in Magenta. Bottom Row: Plots of (5.4)'s $\hat{P}\left\{|\varepsilon_t| \geq 3\hat{\sigma}_\varepsilon | \hat{H}_t, \hat{\Delta}\right\}$ in Red for the SPX, USD/EUR, and BPI with the threshold value for (5.7)'s ξ_t marked in Magenta. \hat{H}_t is the sparse autoregressive model of order 10 defined in (5.1)-(5.2), while $\hat{\Delta}$ is (3.5)'s $\hat{\Delta}(4\hat{\sigma}_\varepsilon)$. The whole-sample results are $\hat{\Delta}_{\text{SPX}} = .28$, $\hat{\Delta}_{\text{USD/EUR}} = .22$, and $\hat{\Delta}_{\text{BPI}} = .39$.

6 Conclusion

We have presented a family of stochastic volatility models that enable dynamic tail inference in heavy-tailed time series. Our explicit results for the models' conditional probabilistic structure allow for straightforward, effective, and computationally inexpensive estimation of model parameters and outcome probabilities. We have shown that this modeling method can be useful for inference of time-varying extreme event probabilities in real time series data. Current and future directions of research involve long-memory modeling for conditionally Laplace processes, accomodation of asymmetric volatility and tails, and generalization of this formalism to the multivariate case.

Acknowledgements

The author thanks Prof. Gennady Samorodnitsky, Cornell University, and Prof. Richard Davis, Columbia University, for their comments on a very early version of this work in 2016. The author is also very grateful to Dr. Dobrislav Dobrev, Federal Reserve Board, for very helpful comments on an early version of this manuscript at the 2017 10th Annual Society for Financial Econometrics (SoFiE) Conference. The author also thanks Prof. Richard Kleeman, Courant Institute of Mathematical Sciences, for many hours of motivating discussions, along with Prof. Fahad Saled, McGill University, and Franz Hinzen, NYU Stern, for encouragement and conversation on these topics. Finally, the author is very grateful to Prof. David Jablons, University of California San Francisco, for his generous encouragement and support.

A Appendix 1: Proofs

A.1 Proof of Lemma 2.1

Proof. We first make the substitution $y = \log(y'/e^{\bar{H}_t})$. Then by (1.2) and (1.4), for $h_t \geq 0$,

$$P(\sigma_t \leq y') = P(h_t \leq y) = \frac{1}{2} - \frac{1}{2} \exp\left(-\frac{\log(e^{-\bar{H}_t} y')}{\Delta}\right) = \frac{1}{2} - \frac{1}{2} \left(\frac{e^{\bar{H}_t}}{y'}\right)^{\frac{1}{\Delta}}$$

We then differentiate w.r.t. y' and let $y' = \sigma_t$, which gives (2.1)'s result for $\sigma_t \geq \exp(\bar{H}_t)$. Next, by (1.2), (1.4), for $h_t < 0$,

$$P(\sigma_t \leq y') = P(h_t \leq y) = \frac{1}{2} \exp\left(\frac{\log(e^{-\bar{H}_t} y')}{\Delta}\right) = \frac{1}{2} \left(\frac{y'}{e^{\bar{H}_t}}\right)^{\frac{1}{\Delta}}.$$

We again differentiate w.r.t. y' and let $y' = \sigma_t$ to give (2.1)'s result for $0 \leq \sigma_t < \exp(\bar{H}_t)$. \square

A.2 Proof of Corollary 2.1

Proof. We note from (2.1) that for any $n \geq 1$, the conditional expected value of σ_t^n is equal to the sum of integrals

$$E\{\sigma_t^n | \mathcal{F}_{t-1}\} = \frac{1}{2\Delta} \left(\exp\left(-\frac{\bar{H}_t}{\Delta}\right) \int_0^{\exp(\bar{H}_t)} \sigma_t^{1/\Delta+n-1} d\sigma_t + \exp\left(\frac{\bar{H}_t}{\Delta}\right) \int_{\exp(\bar{H}_t)}^{\infty} \sigma_t^{-1/\Delta+n-1} d\sigma_t \right),$$

the second term of which diverges for $\Delta \geq 1/n$, while for $\Delta < 1/n$ we have after integration

$$E \{ \sigma_t^n | \mathcal{F}_{t-1} \} = \frac{1}{2} \exp(n\bar{H}_t) \left(\frac{1}{1-n\Delta} + \frac{1}{1+n\Delta} \right) = \frac{\exp(n\bar{H}_t)}{1-n^2\Delta^2}, \quad (\text{A.1})$$

We next note that since z_t is *i.i.d.* and z_t and σ_t are independent, the conditional expectation $E \{ \varepsilon_t^n | \mathcal{F}_{t-1} \} = E z_t^n E \{ \sigma_t^n | \mathcal{F}_{t-1} \}$. Since z_t is standard normal, its n th moment is simply $(n-1)!! = (n-1)(n-3)(n-5)\dots 1$. Therefore $E \{ \varepsilon_t^n | \mathcal{F}_{t-1} \} = (n-1)!! E \{ \sigma_t^n | \mathcal{F}_{t-1} \}$. Using (A.1) then gives (2.2)'s result. \square

A.3 Proof of Theorem 2.1

Proof. We note from Rohatgi (1976 p. 141) that since (1.1)'s z_t and σ_t are independent, the distribution of their product $\sigma_t z_t = \varepsilon_t$ is given by the formula

$$p_\varepsilon(\varepsilon_t | \mathcal{F}_{t-1}) = \int_0^\infty p_\sigma(\sigma_t | \mathcal{F}_{t-1}) p_z\left(\frac{\varepsilon_t}{\sigma_t}\right) \frac{1}{|\sigma_t|} d\sigma_t. \quad (\text{A.2})$$

We then substitute the standard normal density for p_z and (2.1) for p_σ into (A.2) to give

$$\begin{aligned} p_\varepsilon(\varepsilon_t | \mathcal{F}_{t-1}) &= \frac{1}{2\Delta\sqrt{2\pi}} \exp\left(-\frac{\bar{H}_t}{\Delta}\right) \int_0^{\exp(\bar{H}_t)} \sigma_t^{1/\Delta-2} e^{-\frac{\varepsilon_t^2}{2\sigma_t^2}} d\sigma_t \\ &\quad + \frac{1}{2\Delta\sqrt{2\pi}} \exp\left(\frac{\bar{H}_t}{\Delta}\right) \int_{\exp(\bar{H}_t)}^\infty \sigma_t^{-1/\Delta-2} e^{-\frac{\varepsilon_t^2}{2\sigma_t^2}} d\sigma_t \end{aligned} \quad (\text{A.3})$$

We note from (2.5) that the first integral in (A.3) can be written in the following form after simplifying

$$\frac{(\sqrt{2}e^{\bar{H}_t})^{-1/\Delta}}{4\sqrt{\pi}\Delta} |\varepsilon_t|^{1/\Delta-1} \left[\Gamma\left(\frac{1-1/\Delta}{2}, \frac{\varepsilon_t^2}{2\sigma_t^2}\right)_{\sigma_t=e^{\bar{H}_t}} - \Gamma\left(\frac{1-1/\Delta}{2}, \frac{\varepsilon_t^2}{2\sigma_t^2}\right)_{\sigma_t=0} \right] \quad (\text{A.4})$$

To simplify (A.4) further, we note from Abramowitz and Stegun (1965 p. 263) that the upper incomplete gamma function satisfies

$$\Gamma(a, b) \sim b^{a-1} e^{-b} \quad (\text{A.5})$$

as $b \rightarrow \infty$, where \sim indicates that the ratio of the left and right-hand sides tends to 1. Letting $(1-1/\Delta)/2 = a$ and $\varepsilon_t^2/2\sigma_t^2 = b$ in (A.5) shows that the second term in (A.4) vanishes. Final simplification of (A.4) gives the result

$$\frac{1}{4\sqrt{\pi}\Delta} (\sqrt{2}e^{\bar{H}_t})^{-1/\Delta} \Gamma\left(\frac{1-1/\Delta}{2}, \frac{\varepsilon_t^2}{2e^{2\bar{H}_t}}\right) |\varepsilon_t|^{1/\Delta-1}. \quad (\text{A.6})$$

The definition (2.5) can be used again to write the second integral in (A.3) as

$$\frac{(\sqrt{2}e^{\bar{H}_t})^{1/\Delta}}{4\sqrt{\pi}\Delta} |\varepsilon_t|^{-1/\Delta-1} \left[\Gamma\left(\frac{1+1/\Delta}{2}, \frac{\varepsilon_t^2}{2\sigma_t^2}\right)_{\sigma_t=\infty} - \Gamma\left(\frac{1+1/\Delta}{2}, \frac{\varepsilon_t^2}{2\sigma_t^2}\right)_{\sigma_t=e^{\bar{H}_t}} \right] \quad (\text{A.7})$$

after simplifying. The first upper incomplete gamma function term in (A.7) is simply $\Gamma((1+1/\Delta)/2)$. We then note that

$$\Gamma(a) - \Gamma(a, b) = \gamma(a, b). \quad (\text{A.8})$$

Using this identity with (A.7) and simplifying gives

$$\frac{1}{4\sqrt{\pi}\Delta} (\sqrt{2}e^{\bar{H}_t})^{1/\Delta} \gamma\left(\frac{1+1/\Delta}{2}, \frac{\varepsilon_t^2}{2e^{2\bar{H}_t}}\right) |\varepsilon_t|^{-1/\Delta-1}. \quad (\text{A.9})$$

Adding (A.6) and (A.9) gives the result in (2.4). \square

A.4 Proof of Corollary 2.2

Proof. We first note the identity shown in Jameson (2016, 2017)

$$\Gamma(a, b) \sim -\frac{b^a}{a} \quad (\text{A.10})$$

as $b \rightarrow 0$ for $a < 0$. For $\Delta < 1$, $(1 - 1/\Delta)/2 < 0$, and hence using (A.10) and rewriting gives

$$\Gamma\left(\frac{1 - 1/\Delta}{2}, \frac{\varepsilon_t^2}{2e^{2\bar{H}_t}}\right) \sim \frac{2\Delta}{1 - \Delta} \left(\frac{|\varepsilon_t|}{\sqrt{2}e^{\bar{H}_t}}\right)^{1-1/\Delta} \quad (\text{A.11})$$

as $|\varepsilon_t| \rightarrow 0$. We next note the identity

$$\gamma(a, b) \sim \frac{b^a}{a} \quad (\text{A.12})$$

as $b \rightarrow 0$. Using (A.12) and rewriting then gives

$$\gamma\left(\frac{1 + 1/\Delta}{2}, \frac{\varepsilon_t^2}{2e^{2\bar{H}_t}}\right) \sim \frac{2\Delta}{1 + \Delta} \left(\frac{|\varepsilon_t|}{\sqrt{2}e^{\bar{H}_t}}\right)^{1+1/\Delta} \quad (\text{A.13})$$

as $|\varepsilon_t| \rightarrow 0$. Substituting (A.11) and (A.13) into (2.4) and cancelling terms gives

$$p_\varepsilon(\varepsilon_t | \mathcal{F}_{t-1}) \sim \frac{1}{4} \sqrt{\frac{2}{\pi}} \frac{1}{e^{\bar{H}_t}} \left(\frac{1}{1 - \Delta} + \frac{1}{1 + \Delta} \right)$$

as $|\varepsilon_t| \rightarrow 0$, which can be simplified to give the result (2.7). \square

A.5 Proof of Corollary 2.3

Proof. Note that as $|\varepsilon_t| \rightarrow \infty$, by (A.5), the term in (2.4) corresponding to (A.6) converges to a term proportional to

$$\frac{1}{\varepsilon_t^2} \exp\left(-\frac{\varepsilon_t^2}{2e^{2\bar{H}_t}}\right),$$

which vanishes. However, by (2.6), the lower incomplete gamma function satisfies

$$\gamma\left(\frac{1 + 1/\Delta}{2}, \frac{\varepsilon_t^2}{2e^{2\bar{H}_t}}\right) \rightarrow \Gamma\left(\frac{1 + 1/\Delta}{2}\right).$$

Hence as $|\varepsilon_t| \rightarrow \infty$, (2.4) satisfies

$$p_\varepsilon(\varepsilon_t | \mathcal{F}_{t-1}) \sim \frac{1}{4\sqrt{\pi}\Delta} \left(\sqrt{2}e^{\bar{H}_t}\right)^{1/\Delta} \Gamma\left(\frac{1 + 1/\Delta}{2}\right) |\varepsilon_t|^{-1/\Delta-1}, \quad (\text{A.14})$$

which is the limit of the term (A.9). Then we multiply (A.14) by 2 and integrate from Λ to ∞ , which gives the first line of (2.8). We next note from integrating (2.1) with $\Lambda \geq \exp(\bar{H}_t)$ that

$$P\{\sigma_t \geq \Lambda | \mathcal{F}_{t-1}\} = \frac{1}{2} \exp\left(\frac{\bar{H}_t}{\Delta}\right) \Lambda^{-1/\Delta}. \quad (\text{A.15})$$

Comparison with the first line of (2.8) gives the full result. \square

A.6 Proof of Proposition 3.1

Proof. By (1.1) and (1.2), $|\varepsilon_t| = \exp(H_t) |z_t|$. Taking the logarithm gives

$$\log |\varepsilon_t| = H_t + \log |z_t|. \quad (\text{A.16})$$

Since z_t and ε_t are independent, $E \{\log |z_t| | \log |\varepsilon_t|\} = E \log |z_t|$. Then since z_t is standard normal, $z_t^2 \sim \chi^2(1)$. It can then be noted, e.g., from Breidt et. al. (1998) that

$$E \log |z_t| = \frac{1}{2} E \log z_t^2 = \frac{1}{2} \left(\log 2 + \psi \left(\frac{1}{2} \right) \right) = \frac{-\log 2 - \gamma}{2} \approx -.6352, \quad (\text{A.17})$$

where $\psi(x)$ is the *digamma function* (see Abramowitz and Stegun 1965 p. 258-259). Rearranging (A.16), taking the expected value $E \{H_t | \log |\varepsilon_t|\}$, and substituting (A.17) gives the result (3.1). \square

B Appendix 2: The $z_t \sim \text{Lap}(0, 1)$ Case

In this section we briefly show that very similar results to those given in Appendix 1 for (1.1)-(1.4) with $z_t \sim \mathcal{N}(0, 1)$ can be derived for the case where z_t is instead distributed according to the standard Laplace density

$$p_z(z_t) = \frac{1}{2} \exp(-|z_t|), \quad (\text{B.1})$$

which gives $E z_t = 0$ and $E |z_t| = 1$. We first note that an equivalent argument to that in A.2 can be made. We use the fact that (B.1)'s $E z_t^n = n!$ with the result (A.1) to give

$$E \{\varepsilon_t^n | \mathcal{F}_{t-1}\} = \exp(n \bar{H}_t) \frac{n!}{1 - n^2 \Delta^2} \quad (\text{B.2})$$

for even $n \geq 2$. The right hand side of (B.2) with $n = 1$ additionally gives $E \{|\varepsilon_t| | \mathcal{F}_{t-1}\}$.

We next note that an equivalent argument to the one in A.3 can be given, using (2.1) and (B.1) with (A.2) to give an expression composed of two integrals, each of which can be written very similarly to (A.4) and (A.7). Then (A.5) and (A.8) can be used in the same way as above to simplify these terms. Adding these two terms gives the result

$$\begin{aligned} p_\varepsilon(\varepsilon_t | \mathcal{F}_{t-1}) &= \frac{1}{4\Delta} \exp\left(-\frac{\bar{H}_t}{\Delta}\right) \Gamma\left(1 - \frac{1}{\Delta}, \frac{|\varepsilon_t|}{e^{\bar{H}_t}}\right) |\varepsilon_t|^{1/\Delta-1} \\ &\quad + \frac{1}{4\Delta} \exp\left(\frac{\bar{H}_t}{\Delta}\right) \gamma\left(1 + \frac{1}{\Delta}, \frac{|\varepsilon_t|}{e^{\bar{H}_t}}\right) |\varepsilon_t|^{-1/\Delta-1} \end{aligned} \quad (\text{B.3})$$

The identities (A.10) and (A.12) in A.4 can then be used to show that as $|\varepsilon_t| \rightarrow 0$,

$$p_\varepsilon(\varepsilon_t | \mathcal{F}_{t-1}) \sim \frac{1}{2e^{\bar{H}_t}} \frac{1}{1 - \Delta^2}. \quad (\text{B.4})$$

The argument in A.5 can also be repeated for $|\varepsilon_t| \rightarrow \infty$, using (A.5) to show that (B.3)'s first term vanishes, and then noting (2.6)'s definition to give

$$p_\varepsilon(\varepsilon_t | \mathcal{F}_{t-1}) \sim \frac{1}{4\Delta} \exp\left(\frac{\bar{H}_t}{\Delta}\right) \Gamma\left(1 + \frac{1}{\Delta}\right) |\varepsilon_t|^{-1/\Delta-1} \quad (\text{B.5})$$

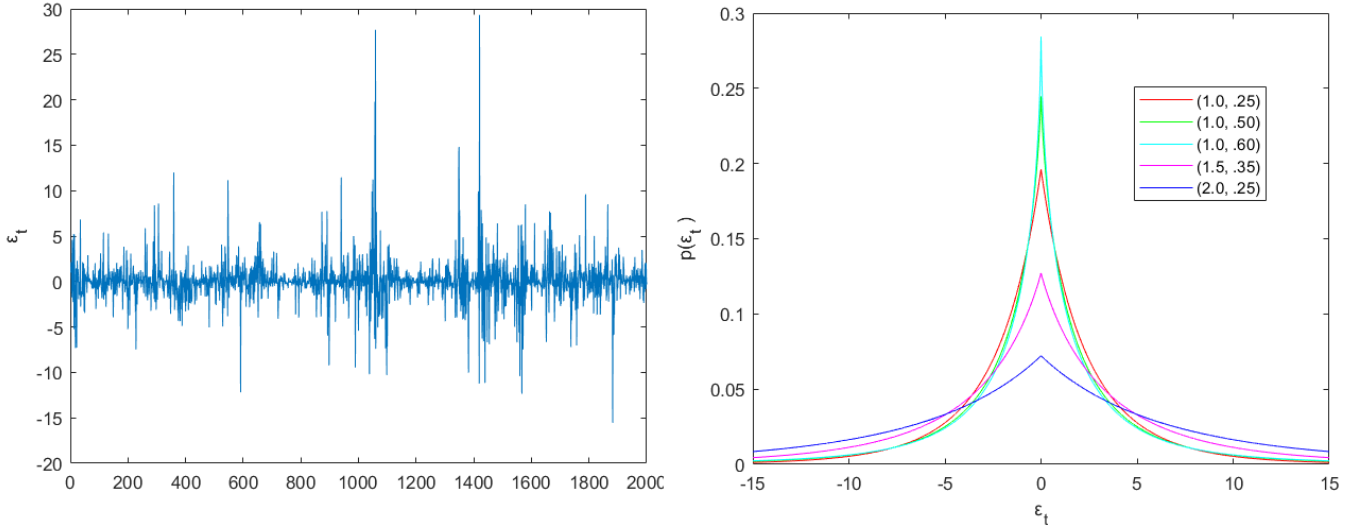


Figure 5: Left: A typical realization of the process ε_t defined in (1.1)-(1.4) with $z_t \sim \text{Lap}(0,1)$, $H_t = .5H_{t-1} + .4H_{t-2} + h_t$, and $\Delta = 1/4$. Right: Graphs of the probability density functions (B.3) with (\bar{H}_t, Δ) equal to (1, .25) in Red, (1, .50) in Green, (1, .60) in Cyan, (1.5, .35) in Magenta, and (2, .25) in Blue.

Then multiplying (B.5) by 2, integrating from Λ to ∞ , and recalling (A.15) gives

$$\begin{aligned} P\{|\varepsilon_t| \geq \Lambda | \mathcal{F}_{t-1}\} &\sim \frac{1}{2} \Gamma\left(1 + \frac{1}{\Delta}\right) \exp\left(\frac{\bar{H}_t}{\Delta}\right) \Lambda^{-1/\Delta} \\ &= \Gamma\left(1 + \frac{1}{\Delta}\right) P\{\sigma_t \geq \Lambda | \mathcal{F}_{t-1}\}. \end{aligned} \quad (\text{B.6})$$

Since $\Gamma(1) = \Gamma(2) = 1$, (B.6)'s second line reduces to $P\{|\varepsilon_t| \geq \Lambda | \mathcal{F}_{t-1}\} \sim P\{\sigma_t \geq \Lambda | \mathcal{F}_{t-1}\}$ for $\Delta = 1$ and as $\Delta \rightarrow \infty$. Several graphs of (B.3) are given in Fig. 5.

C Appendix 3: Non-Financial Empirical Applications

The stochastic volatility formalism described in Section 1-3 can be applied to non-financial time series as well. In this section we apply this modeling to two data sets respectively concerned with urban air pollution and solar activity. The first data set is the levels of PM2.5 particulate matter concentration (in $\mu\text{g}/\text{m}^3$) measured hourly at the U.S. Embassy in Beijing from January 1st, 2010 to December 31st, 2014 (see Liang et. al. 2015). A linear AR(44) model is fitted to the levels using the Yule-Walker method, with order selected using the Akaike Information Criterion (AIC). We then apply Section 1-3's modeling to the AR(44) model's corresponding residuals, using 41,665 samples over approximately 5 years. The second data set is monthly sunspot numbers observed from January, 1749 to July, 2014, retrieved from the Royal Observatory of Belgium. We similarly use Yule-Walker and AIC to fit a linear AR(29) model to the sunspot numbers. We then apply Section 1-3's modeling to the AR(29) model's corresponding residuals, using 3,124 samples over approximately 261 years. Hence for both applications we are using Section 1-3's formalism to model the fluctuations in the data that are not captured by the linear autoregressive models.

We apply the same L1-penalized Principal Component Regression method for (3.3)'s \hat{H}_t as described in Section 5. However, we use $\left\{\hat{H}_{t-1}, \dots, \hat{H}_{t-48}\right\}_{t=49}^{T+48}$ for the Beijing PM2.5 data, giving its

Table 3: Non-Financial Application Results:

Averages are calculated from 100 random train/test splits for each row.

Beijing PM2.5						
$N_{\text{Train}}/N_{\text{Test}}$		avg. $\widehat{\Delta}(4\widehat{\sigma}_\varepsilon)$	avg. $\rho_{ \varepsilon ,\widehat{\sigma}}$	avg. $\rho_{ \varepsilon ,\widehat{P}}$	avg. Sn.	avg. Sp.
20,832/20,833	(50/50)	.445	.326	.315	.827	.595
24,999/16,666	(60/40)	.449	.328	.321	.831	.594
29,165/12,500	(70/30)	.438	.329	.313	.818	.602
33,332/8,333	(80/20)	.442	.332	.321	.823	.598
37,498/4,167	(90/10)	.429	.333	.313	.810	.613
Sunspots						
$N_{\text{Train}}/N_{\text{Test}}$		avg. $\widehat{\Delta}(4\widehat{\sigma}_\varepsilon)$	avg. $\rho_{ \varepsilon ,\widehat{\sigma}}$	avg. $\rho_{ \varepsilon ,\widehat{P}}$	avg. Sn.	avg. Sp.
1,562/1,562	(50/50)	.180	.343	.242	.829	.741
1,874/1,250	(60/40)	.184	.348	.245	.834	.741
2,186/938	(70/30)	.175	.349	.237	.837	.742
2,499/625	(80/20)	.179	.351	.244	.845	.743
2,811/313	(90/10)	.175	.348	.240	.858	.743

model for \widehat{H}_t a memory length of 48 hours. For the sunspot data, we use $\left\{\widehat{H}_{t-1}, \dots, \widehat{H}_{t-24}\right\}_{t=25}^{T+24}$, giving its model for \widehat{H}_t a memory length of 24 months. We again use (3.5)'s $\widehat{\Delta} = \widehat{\Delta}(4\widehat{\sigma}_\varepsilon)$, and we study the volatility and dynamic probability estimates (5.3)-(5.4) as well as the binary classifier (5.7). We give the empirical results $\widehat{\Delta}(4\widehat{\sigma}_\varepsilon)$, the testing correlations (5.5)-(5.6), and the testing sensitivity (5.8) and specificity (5.9) in Table 3. The results are averaged over 100 random train/test splits for several different ratios of training sample size to testing sample size.

First note from Table 3 that the PM2.5 residuals are estimated to have much heavier tails than the financial time series in Section 5, with $\widehat{\Delta}$ ranging from .43 to .45. For the Beijing PM2.5 data, the classifier ξ_t exhibits test sensitivity of 81% to 83%, which is accompanied by a specificity of about 60%. This gives a balanced accuracy of about 71%. Additionally, the PM2.5 data's average test correlations $\rho_{|\varepsilon|,\widehat{\sigma}}$ and $\rho_{|\varepsilon|,\widehat{P}}$ are about 33% and 32% respectively.

We next note from Table 3 that the sunspot residuals are estimated to have much lighter tails than the PM2.5 residuals, with $\widehat{\Delta} \approx .18$. The sunspot data's classifier ξ_t exhibits test sensitivity and specificity of about 84% and 74% respectively, giving a high balanced accuracy of about 79%. The sunspot data's average test correlations $\rho_{|\varepsilon|,\widehat{\sigma}}$ and $\rho_{|\varepsilon|,\widehat{P}}$ are about 35% and 24% respectively.

These results show strong predictiveness on the test sets for both applications. However, we note that since the AR(44) and AR(29) models were calibrated over the entire data sets, there is potentially information from the test sets embedded within the training sets. Nevertheless, these applications show that Section 1-3's methodology has great flexibility and can be useful for nonlinear, heavy-tailed time series modeling in many fields. Plots of the Beijing PM2.5 and sunspot data along with corresponding volatility and probability estimates are given in Fig. 6.

SUPPLEMENTARY MATERIAL

R scripts: R scripts containing code to perform the simulation studies in Section 4 and the empirical applications in Section 5 and Appendix 3. (.R files)

Data sets: Data sets used in the empirical applications in Section 5 and Appendix 3. (.xlsx files)
For supplementary materials email gordon.chavez@ucsf.edu.

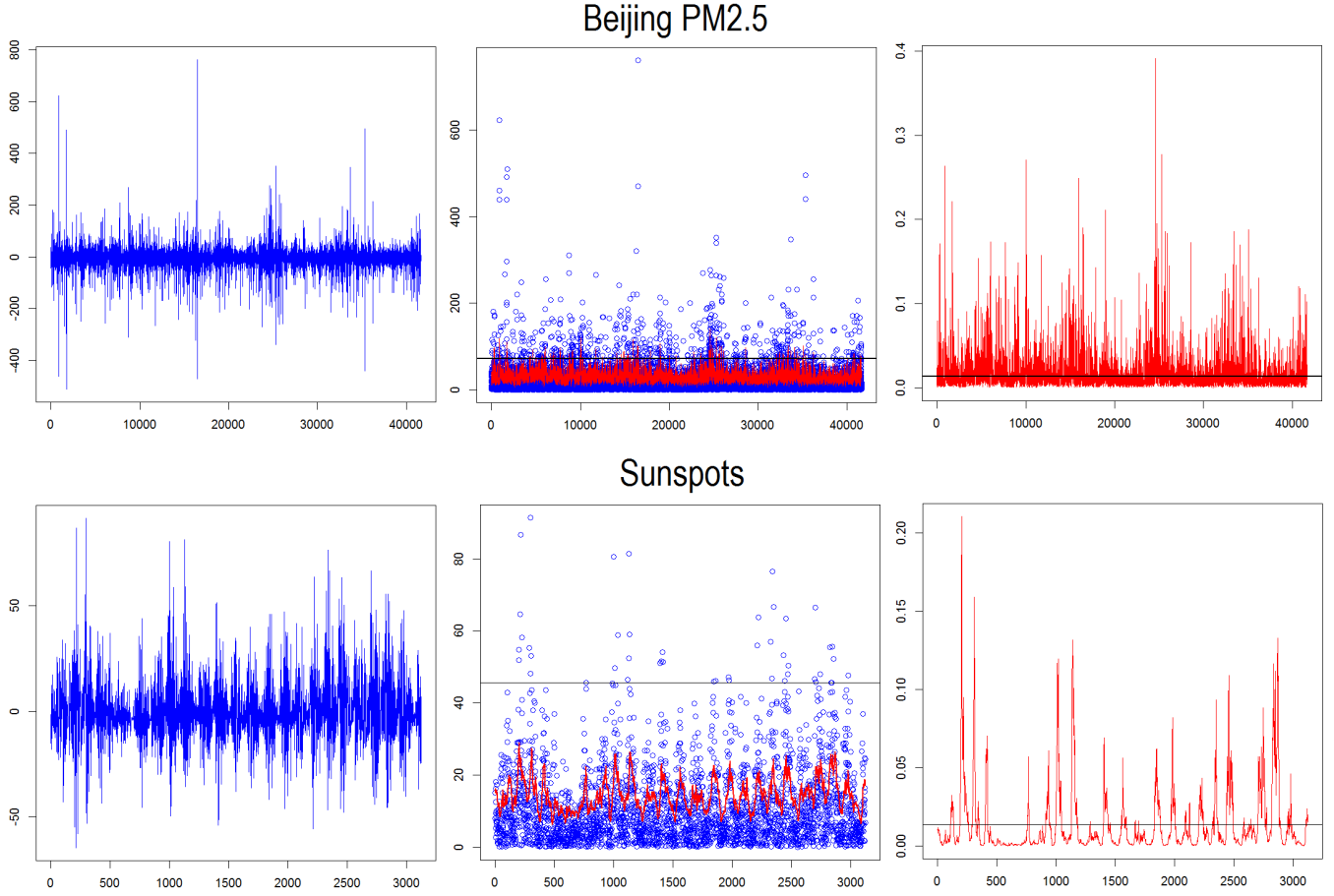


Figure 6: Top: Beijing PM2.5 Application. Bottom: Sunspots Application.

Left: Plots of the AR model residuals ε_t . Middle: Plots of $|\varepsilon_t|$ in Blue and (5.3)'s $\hat{\sigma}_{\varepsilon,t}$ in Red with $3\hat{\sigma}_\varepsilon$ marked in Black. Right: Plots of (5.4)'s $\hat{P}\left\{|\varepsilon_t| \geq 3\hat{\sigma}_\varepsilon | \hat{H}_t, \hat{\Delta}\right\}$ in Red with the threshold value for (5.7)'s ξ_t marked in Black. \hat{H}_t is a sparse autoregressive model of order 48 (Top) and order 24 (Bottom), while $\hat{\Delta}$ is given by (3.5)'s $\hat{\Delta}(4\hat{\sigma}_\varepsilon)$. The whole-sample results are $\hat{\Delta}_{\text{Beijing PM2.5}} = .45$ and $\hat{\Delta}_{\text{Sunspots}} = .20$.

References

- [1] Abramowitz, M. and I.A. Stegun (Editors) (1965). Handbook of Mathematical Functions. Dover. New York, NY.
- [2] Andersen, T.G., T. Bollerslev, F.X. Diebold, and P. Labys (2001). The distribution of realized exchange rate volatility. *Journal of the American Statistical Association* 96(453), 42-55.
- [3] Ardia, D. (2008). Financial Risk Management with Bayesian Estimation of GARCH Models. *Lecture Notes in Economics and Mathematical Systems* 612. Springer-Verlag. Berlin, Heidelberg.
- [4] Ardia, D. and L.F. Hoogerheide (2010). Bayesian estimation of the GARCH(1,1) model with Student-t innovations. *The R Journal* 2(2), 41-47.
- [5] Black, F. (1976). Studies of stock price volatility changes. *Proceedings of the 1976 Meetings of the American Statistical Association*, 171-181.
- [6] Board of Governors of the U.S. Federal Reserve System (2018). U.S. / Euro Foreign Exchange Rate retrieved from FRED, Federal Reserve Bank of St. Louis; <https://fred.stlouisfed.org/series/DEXUSEU>.
- [7] Bollerslev, T. (1986). Generalized autoregressive conditional heteroskedasticity. *Journal of Econometrics* 31(3), 307-327.
- [8] Bollerslev, T. and H.O. Mikkelsen (1996). Modeling and pricing long memory in stock market volatility. *Journal of Econometrics* 73(1), 151-184.
- [9] Breidt, F.J., N. Crato, and P. de Lima (1998). The detection and estimation of long memory in stochastic volatility. *Journal of Econometrics* 83(1-2), 325-348.
- [10] Chib, S., F. Nardari, and N. Shephard (2002). Markov chain Monte Carlo methods for stochastic volatility models. *Journal of Econometrics* 108(2), 281-316.
- [11] Christie, A.A. (1982). The stochastic behavior of common stock variances: value, leverage, and interest rate effects. *Journal of Financial Economics* 10(4), 407-432.
- [12] deHaan, L. and S.I. Resnick (1980). A simple asymptotic estimate for the index of a stable distribution. *Journal of the Royal Statistical Society Series B* 42(1), 83-87.
- [13] Diebold, F.X., T. Schuermann, and J.D. Stroughair (2000). Pitfalls and opportunities in use of extreme value theory in risk management. *Journal of Risk Finance* 1(2), 30-35.
- [14] Ding, Z., C.W.J. Granger, and R.F. Engle (1993). A long memory property of stock market returns and a new model. *Journal of Empirical Finance* 1(1), 83-106.
- [15] Embrechts, P., C. Kluppelberg, and T. Mikosch (2011). Modelling Extremal Events for Insurance and Finance. Springer. Heidelberg.
- [16] Engle, R.F. (1982). Autoregressive conditional heretoskedasticity with estimates of the variance of United Kingdom inflation. *Econometrica* 50(4), 987-1007.
- [17] Engle, R.F. and V.K. Ng (1993). Measuring and testing the impact of news on volatility. *Journal of Finance* 48(5), 1749-1778.

- [18] Fama, E.F. and R. Roll (1968). Some properties of symmetric stable distributions. *Journal of the American Statistical Association* 63(323), 817-836.
- [19] Friedman, J., T. Hastie, and R. Tibshirani (2010). Regularization paths for generalized linear models via coordinate descent. *Journal of Statistical Software* 33(1), 1-22.
- [20] Gardes, L. and S. Girard (2008). A moving window approach for nonparametric estimation of the conditional tail index. *Journal of Multivariate Analysis* 99(10), 2368-2388.
- [21] Gardes, L. and G. Stupfler (2014). Estimation of the conditional tail index using a smoothed local Hill estimator. *Extremes* 17(1), 45-75.
- [22] Gencay, R., F. Selcuk, and B. Whitcher (2001). Scaling properties of foreign exchange volatility. *Physica A: Statistical Mechanics and its Applications* 289(1), 249-266.
- [23] Grau-Carles, P. (2000). Empirical evidence of long-range correlations in stock returns. *Physica A: Statistical Mechanics and its Applications* 287(3-4), 396-404.
- [24] Harvey, A.C., E. Ruiz, and N. Shephard (1994). Multivariate stochastic variance models. *Review of Economic Studies* 61(2), 247-264.
- [25] Hill, B.M. (1975). A simple general approach to inference about the tail of a distribution. *Annals of Statistics* 3(5), 1163-1174.
- [26] Jacquier, E., N.G. Polson, and P.E. Rosse (1994). Bayesian analysis of stochastic volatility models. *Journal of Business & Economic Statistics* 12(4), 371-389.
- [27] Jameson, G.J.O. (2016). The incomplete gamma functions. *The Mathematical Gazette* 100(548), 298-306.
- [28] Jameson, G.J.O. (2017). The incomplete gamma functions (notes); <https://www.maths.lancs.ac.uk/jameson/gammainc.pdf>.
- [29] Johnson, N.L., S. Kotz, and N. Balakrishnan (1994). Continuous Univariate Distributions Vol. 1. 14: Lognormal Distributions. Wiley. New York, NY.
- [30] Kearns, P. and A. Pagan (1997). Estimating the density tail index for financial time series. *The Review of Economics and Statistics* 79(2), 171-175.
- [31] Kelly, B. (2014) The dynamic power law model. *Extremes* 17(4), 557-583.
- [32] Kim, S., N. Shephard, and S. Chib (1998). Stochastic volatility: likelihood inference and comparison with ARCH models. *Review of Economic Studies* 65(3), 361-393.
- [33] Liang, X., T. Zou, B. Guo, S. Li, H. Zhang, S. Zhang, H. Huang, and S.X. Chen (2015). Assessing Beijing's PM2.5 pollution: severity, weather impact, APEC and winter heating. *Proceedings of the Royal Society A* 471(2182).
- [34] Liesenfeld, R. and R.C. Jung (2000). Stochastic volatility models: conditional normality versus heavy-tailed distributions. *Journal of Applied Econometrics* 15(2), 137-160.
- [35] Lobato, I.N. and N.E. Savin (1998). Real and spurious long-memory properties of stock-market data. *Journal of Business & Economic Statistics* 16(3), 261-268.

- [36] Mandelbrot, B.B. (1963). The variation of certain speculative prices. *Journal of Business* 36(4), 394-419.
- [37] McNeil, A.J. and R. Frey (2000). Estimation of tail-related risk measures for heteroscedastic financial time series: an extreme value approach. *Journal of Empirical Finance* 7(3-4), 271-300.
- [38] Mousazadeh, S. and M. Karimi (2007). Parameter estimation for Student-t ARCH model using MDL criterion. *2007 IEEE International Conference on Signal Processing and Communications*.
- [39] Nelson, D.B. (1991). Conditional heteroskedasticity in asset returns: a new approach. *Econometrica* 59(2), 347-370.
- [40] Pickands, J. (1975). Statistical inference using extreme order statistics. *Annals of Statistics* 3(1), 119-131.
- [41] Ray, B.K. and R.S. Tsay (2000). Long-range dependence in daily stock volatilities. *Journal of Business & Economic Statistics* 18(2), 254-262.
- [42] Rohatgi, V.K. (1976). An Introduction to Probability Theory and Mathematical Statistics. Wiley. New York, NY.
- [43] Sandmann, G. and S.J. Koopman (1998). Estimation of stochastic volatility models via Monte Carlo maximum likelihood. *Journal of Econometrics* 87(2), 271-301.
- [44] Taylor, S.J. (1982). Financial returns modelled by the product of two stochastic processes—a study of daily sugar prices 1961-1979. In Anderson, O.D. (Editor), *Time Series Analysis: Theory and Practice*, Vol. 1. Amsterdam, North-Holland. 203-226.
- [45] Taylor, S.J. (1986). *Modeling Financial Time Series*. Wiley. Chichester.
- [46] Terasvirta, T., D. Tjøstheim, and C.W.J. Granger (2010). *Modelling Nonlinear Economic Time Series*. Oxford. New York.
- [47] Tibshirani, R. (1996). Regression shrinkage and selection via the Lasso. *Journal of the Royal Statistical Society. Series B* 58(1), 267-288.
- [48] WDC-SILSO, Solar Influences Data Analysis Center (SIDC), Royal Observatory of Belgium, Av. Circulaire, 3, B-1180 BRUSSELS; <http://www.sidc.be/silso/datafiles>.